

# On the decay of two-dimensional homogeneous turbulence

J. R. Chasnov<sup>a)</sup>

The Hong Kong University of Science and Technology, Clear Water Bay, Kowloon, Hong Kong

(Received 19 June 1996; accepted 3 September 1996)

Direct numerical simulations of decaying two-dimensional turbulence in a fluid of large extent are performed primarily to ascertain the asymptotic decay laws of the energy and enstrophy. It is determined that a critical Reynolds number  $R_c$  exists such that for initial Reynolds numbers with  $R(0) < R_c$  final period of decay solutions result, whereas for  $R(0) > R_c$  the flow field evolves with increasing Reynolds number. Exactly at  $R(0) = R_c$ , the turbulence evolves with constant Reynolds number and the energy decays as  $t^{-1}$  and the enstrophy as  $t^{-2}$ . A  $t^{-2}$  decay law for the enstrophy was originally predicted by Batchelor for large Reynolds numbers [Phys. Fluids Suppl. II, **12**, 233 (1969)]. Numerical simulations are then performed for a wide range of initial Reynolds numbers with  $R(0) > R_c$  to study whether a universal power-law decay for the energy and enstrophy exist as  $t \rightarrow \infty$ . Different scaling laws are observed for  $R(0)$  moderately larger than  $R_c$ . When  $R(0)$  becomes sufficiently large so that the energy remains essentially constant, the enstrophy decays at large times as approximately  $t^{-0.8}$ . © 1997 American Institute of Physics. [S1070-6631(96)01912-5]

## I. INTRODUCTION

We consider here the decay of a two-dimensional homogeneous turbulence in a fluid of infinite extent. One of the attractions of studying two-dimensional turbulence is its computational simplicity with respect to fully developed three-dimensional turbulence. Nevertheless, numerical simulations are still non-trivial, requiring high resolution and long-time integrations, and the asymptotic behavior of the statistics during the decay remains an open problem.

The main contribution of this paper is to present some new direct numerical simulation results for decaying two-dimensional turbulence. Particular emphasis is placed on determining the long-time asymptotic evolution of the energy and enstrophy as a function of the initial Reynolds number of the flow field. We consider here the asymptotic statistical evolution of the flow field without specifically confronting the existence of coherent vortices or their intermittent distribution in the fluid. This is counter to most current trends in two-dimensional turbulence research.<sup>1-3</sup> Nevertheless, we feel that a careful study of the dependence of the decay statistics on the initial Reynolds number of the turbulence may yield some useful information about the physics of the decay.

We arrive at our study of two-dimensional turbulence through earlier work on decaying three-dimensional isotropic turbulence.<sup>4</sup> In this previous study, large-eddy simulations were used to confirm theoretical predictions of asymptotic decay laws for the energy and the self-similar decay of the energy spectrum based on low wave number spectral invariants. The higher resolutions obtainable in simulations of two-dimensional turbulence permit a study of two-dimensional decay at relatively high Reynolds numbers by direct numerical simulations without the need for subgrid scale modeling.

To place our simulation results within some general

theoretical framework, it is worthwhile first to review an argument of Batchelor's<sup>5</sup> concerning the decay, as well as some related later developments.<sup>6,7</sup> The Navier–Stokes equations for two-dimensional turbulence independent of the third direction with velocity field  $\mathbf{u} = (u_1, u_2, 0)$  and vorticity field  $\boldsymbol{\omega} = (0, 0, \omega)$  may be written as

$$\frac{\partial \boldsymbol{\omega}}{\partial t} + \nabla \cdot (\mathbf{u} \boldsymbol{\omega}) = \nu \nabla^2 \boldsymbol{\omega}, \quad (1)$$

where

$$\boldsymbol{\omega} = \nabla \times \mathbf{u}, \quad \text{and} \quad \nabla \cdot \mathbf{u} = 0. \quad (2)$$

From (1) and (2), time-evolution equations for the mean-square velocity ( $2 \times$  energy)  $\langle \mathbf{u}^2 \rangle$  and mean-square vorticity ( $2 \times$  enstrophy)  $\langle \omega^2 \rangle$  are determined to be

$$\frac{d}{dt} \langle \mathbf{u}^2 \rangle = -2\nu \langle \omega^2 \rangle, \quad (3)$$

and

$$\frac{d}{dt} \langle \omega^2 \rangle = -2\nu \langle (\nabla \omega)^2 \rangle. \quad (4)$$

These equations are exact but unclosed because of the presence of the mean-square gradient of the vorticity ( $2 \times$  palinstrophy) on the right-hand side of (4).

Batchelor considered the limit  $\nu \rightarrow 0$  of (3) and (4). Since from Eq. (4) the enstrophy is bounded by its initial value, one has from Eq. (3) at a fixed time  $t$ ,  $d\langle \mathbf{u}^2 \rangle/dt \rightarrow 0$ , or  $\langle \mathbf{u}^2 \rangle \rightarrow u_0^2$ , its initial value. This is in contrast to the decay of a three-dimensional turbulence where the zero viscosity limit is thought to be singular, and there exists some critical time at infinite Reynolds number, before which the energy remains constant and after which the energy decays as a power law.<sup>8</sup>

Batchelor then proposed that Eq. (4) may be singular in the limit  $\nu \rightarrow 0$  in that the time derivative of the enstrophy may not vanish in this limit. Furthermore, the existence of

<sup>a)</sup>Phone: (852) 23587448; Fax: (852) 23581643; Electronic mail: machas@uxmail.ust.hk

$u_0$  as an invariant of the fluid motion led Batchelor to suggest the hypothesis of a self-similar decay based on  $u_0$ . Dimensional analysis then requires all statistics to scale on  $u_0$  and  $t$  alone, and considering the units of enstrophy one obtains immediately  $\langle \omega^2 \rangle \propto t^{-2}$ . Although not stated explicitly, the Batchelor argument thus implies the existence of a critical time  $t_c$  in two-dimensional turbulence at infinite Reynolds number ( $\nu \rightarrow 0$ ) at which the palinstrophy diverges. For  $t < t_c$  the enstrophy is constant, whereas for  $t > t_c$  the enstrophy decays as  $t^{-2}$ . The energy remains constant over the entire decay.

However, subsequent work<sup>6,7</sup> on two-dimensional turbulence decay has shown that there exists no finite time singularities for this flow. That is, for any fixed time  $t$  the time derivatives of both the energy and enstrophy vanish as  $\nu \rightarrow 0$ . Nevertheless, even though Batchelor's results apparently do not apply for fixed  $t$  as  $\nu \rightarrow 0$ , it was proposed on the basis of closure calculations<sup>7,8</sup> that they remain valid for fixed but small  $\nu$  as  $t \rightarrow \infty$ . The critical time  $t_c$  after which enstrophy is dissipated is now a (slowly) increasing function of the initial Reynolds number.

Given the approximate very high Reynolds number enstrophy decay law

$$\langle \omega^2 \rangle = \begin{cases} \omega_0^2, & \text{if } t < t_c, \\ \omega_0^2 (t_c/t)^2 & \text{if } t > t_c, \end{cases} \quad (5)$$

where  $\omega_0^2$  is the initial mean-square vorticity of the fluid, Eq. (3) may be integrated for the energy. One obtains for the energy decay:

$$\langle u^2 \rangle = \begin{cases} u_0^2 - 2\nu\omega_0^2 t, & \text{if } t < t_c, \\ u_0^2 - 4\nu\omega_0^2 t_c [1 - \frac{1}{2}(t_c/t)] & \text{if } t > t_c. \end{cases} \quad (6)$$

The decay law of the enstrophy given by (5) thus results in an energy which decays from its initial value of  $u_0^2$  to a final value ( $t \rightarrow \infty$ ) of  $u_*^2 = u_0^2 - 4\nu\omega_0^2 t_c$ . This implies that an amount of energy equal to  $u_*^2$  must eventually escape the effect of viscosity by moving to larger-and-larger scales, asymptotically approaching wave number zero in spectral space on which viscosity no longer acts.

The outline of the remainder of our paper is as follows. In Section II we will briefly discuss the novel features of our numerical method. In Section III we will present some numerical results at low Reynolds number for which it will be possible to obtain a clear and simple theoretical description. In Section IV high Reynolds number results for the decay of the energy and enstrophy will be presented. These will be further analyzed in Section V and various scaling laws for different ranges of initial Reynolds numbers will be postulated which are in agreement with the simulation data. Finally, in Section VI the self-similar decay of the energy spectrum will be considered.

## II. NUMERICAL METHOD

Our numerical method time advances the Fourier coefficients of the vorticity field treating the viscous term in (1) as

an integrating factor. Denoting the Fourier coefficients with carets and the wave number components by  $k_1, k_2$ , with  $k^2 = k_1^2 + k_2^2$ , the transform of (1) yields

$$\frac{\partial}{\partial t} [\widehat{\omega} \exp(\nu k^2 t)] = -\exp(\nu k^2 t) \nabla \cdot (\widehat{\mathbf{u}} \mathbf{\omega}), \quad (7)$$

where the convection term on the right-hand side may be rewritten using (2) as

$$-\nabla \cdot (\widehat{\mathbf{u}} \mathbf{\omega}) = k_1 k_2 (\widehat{u_2^2} - \widehat{u_1^2}) - (k_2^2 - k_1^2) \widehat{u_1} \widehat{u_2}. \quad (8)$$

The Fourier components of the velocity field are determined from the vorticity field using

$$\widehat{u_1} = i \frac{k_2}{k^2} \widehat{\omega}, \quad \widehat{u_2} = -i \frac{k_1}{k^2} \widehat{\omega}. \quad (9)$$

Equation (7) is time integrated using the standard fourth-order Runge-Kutta method with variable time step  $\Delta t$  determined by the Courant-Friedrichs-Lewy condition

$$\Delta t = \frac{C}{2\pi} \frac{\Delta}{\max[|u_1| + |u_2|]}, \quad (10)$$

where  $\Delta$  is the grid spacing in both directions and  $\max[\dots]$  indicates the maximum value attained over all the grid points. Minimization of ones computer cost requires maximizing the value of  $C$  and after some numerical experimentation we have determined that  $C = 10$  yields sufficient accuracy. The nonlinear convective term in (8) is evaluated by forming the Fourier coefficients of the velocity field using (9), transforming to physical space and forming the products  $u_1 u_2$  and  $u_2^2 - u_1^2$ , and then transforming back to Fourier space. Hence only four two-dimensional fast Fourier transforms (FFTs) are required to compute the nonlinear term, whereas direct evaluation of the left-hand side of (8) requires one additional FFT.<sup>9</sup> The entire calculation is dealiased using a circular truncation of Fourier modes with wave number magnitude greater than  $N/3$ , where  $N$  is the number of grid points in each direction. Such a dealiasing ensures exact conservation of energy and enstrophy by the numerical method with vanishing viscosity. A parallel simulation code for the Intel Paragon originally developed by Rogallo and Wray<sup>10</sup> for three-dimensional turbulence and used in our earlier study<sup>4</sup> was rewritten to solve (7) efficiently.

We specify initial conditions for our flow field by assuming an energy spectrum of wave number magnitude  $k$  of the general form

$$E(k, 0) = \frac{1}{2} a_s u_0^2 k_p^{-1} \left( \frac{k}{k_p} \right)^{2s+1} \exp \left[ - \left( s + \frac{1}{2} \right) \left( \frac{k}{k_p} \right)^2 \right] \quad (11)$$

with  $s = 0, 1, 2, \dots$ , and where the normalization constant  $a_s$  is given by

$$a_s = (2s + 1)^{s+1} / 2^s s!$$

All the results presented here correspond to  $s = 3$ . This allows the development of a  $k^3$  energy spectrum at small wave numbers<sup>8</sup> to be a consequence of the non-linear interactions among different Fourier components of the flow field. The

initial vorticity field is generated in Fourier space with random phases and with amplitude corresponding to (11), i.e.,

$$\hat{\omega}(\mathbf{k},0) = \left( \frac{kE(k,0)}{\pi} \right)^{1/2} \exp(i2\pi\xi), \quad (12)$$

with  $\xi$  a different uniform deviate for each wave number vector  $\mathbf{k}$  subject to the requirement of complex conjugate symmetry of the Fourier components.

Given the form of the initial energy spectrum (11) with  $s=3$ , a simulation run is uniquely identified by its (micro-scale) Reynolds number  $R(t)$  at  $t=0$ , where we define the Reynolds number at time  $t$  by

$$R(t) = \frac{ul}{\nu}, \quad (13)$$

with

$$u(t) = \langle u^2 \rangle^{1/2}, \quad \omega(t) = \langle \omega^2 \rangle^{1/2}, \quad l(t) = u(t)/\omega(t). \quad (14)$$

The value of  $u(t)$ ,  $\omega(t)$  and  $l(t)$  at  $t=0$  is determined from the initial energy spectrum (11) to be

$$u(0) = u_0, \quad \omega(0) \equiv \omega_0 = \sqrt{\frac{2s+2}{2s+1}} u_0 k_p, \quad (15)$$

$$l(0) \equiv l_0 = \sqrt{\frac{2s+1}{2s+2}} k_p^{-1},$$

so that with  $s=3$ , one has

$$R(0) = \sqrt{\frac{7}{8}} \frac{u_0}{k_p \nu}. \quad (16)$$

The maximum number of grid points used in the simulations is  $4096^2$ .

### III. THE DECAY AT LOW REYNOLDS NUMBERS

We first consider the evolution of the flow field at relatively low initial Reynolds numbers. Batchelor's high Reynolds number result of constant energy and an enstrophy decreasing as  $t^{-2}$  implies that the Reynolds number of the turbulence at time  $t$  given by (13) increases linearly in time. However, well-known ideas concerning the final period of decay of a turbulent flow field implies a Reynolds number which decreases in time. We thus postulate the existence of a critical initial Reynolds number above which the Reynolds number of the turbulence increases asymptotically, and below which it decreases to small values eventually attaining the final period of decay.

An analysis of the final period of decay in two-dimensional turbulence follows closely the three-dimensional case. It is assumed that during the early time evolution, nonlinear interactions are sufficiently strong so that the energy spectrum after some time  $t$  takes the low-wave-number form<sup>8</sup>

$$E(k,t) \sim \pi B_2(t) k^3, \quad k \rightarrow 0, \quad (17)$$

as a consequence of direct nonlinear transfer of energy from small-to-large scales, commonly called backscatter. At subsequent times, it is further assumed that the Reynolds num-

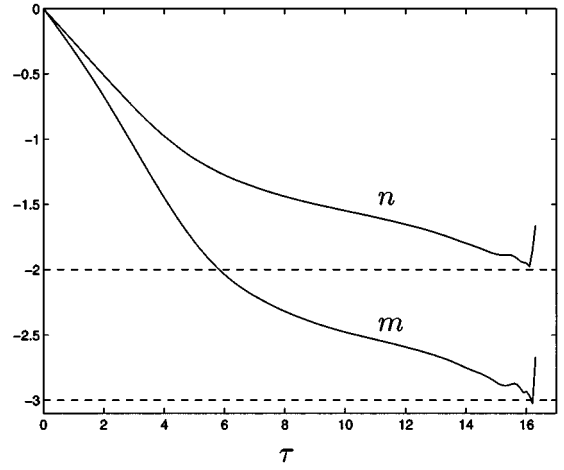


FIG. 1. Evolution of the logarithmic derivative of the energy ( $n$ ) and enstrophy ( $m$ ) for  $R(0)=8$ .

ber has decayed sufficiently so that the nonlinear terms in the governing equation are negligible and the coefficient  $B_2$  in (17) becomes constant. The linear governing equations may then be integrated exactly and one obtains the following final period of decay solutions for the energy and enstrophy as  $t \rightarrow \infty$ :

$$\langle \mathbf{u}^2 \rangle \propto B_2(\nu t)^{-2}, \quad \langle \omega^2 \rangle \propto B_2(\nu t)^{-3}. \quad (18)$$

Such a solution may also be obtained from dimensional analysis by requiring the energy and enstrophy to be linearly dependent on  $B_2$  as a consequence of the linearity of the equations, and in addition to be functions of  $\nu$  and  $t$  alone.<sup>4</sup> The Reynolds number of the turbulence during the final period is found to decrease as  $t^{-1/2}$  so that this solution is internally consistent.

Results for the energy and enstrophy decay from direct numerical simulations performed with initial Reynolds number  $R(0)=8$  are presented in Fig. 1. To best test the theoretical results, we define the logarithmic derivative in time of the energy and enstrophy as

$$n = \frac{d \ln \langle \mathbf{u}^2 \rangle}{d \ln t}, \quad m = \frac{d \ln \langle \omega^2 \rangle}{d \ln t}, \quad (19)$$

which may be computed using (3) and (4) from

$$n = -2\nu t \frac{\langle \omega^2 \rangle}{\langle \mathbf{u}^2 \rangle}, \quad m = -2\nu t \frac{\langle (\nabla \omega)^2 \rangle}{\langle \omega^2 \rangle}. \quad (20)$$

If the energy and enstrophy decay as power laws in time, then their logarithmic derivatives are just the power-law exponents. In Fig. 1, the logarithmic derivatives  $n$  and  $m$  are plotted versus  $\tau$ , where

$$\tau = \int_0^t dt \langle \omega^2 \rangle^{1/2} \quad (21)$$

can be considered a measure of the number of eddy turnover times undergone by the flow at time  $t$ . The normalized time  $\tau$  best represents the time interval over which one expects significant changes in the power-law exponent. It is apparent from Fig. 1 that the final period of decay solution (18) is

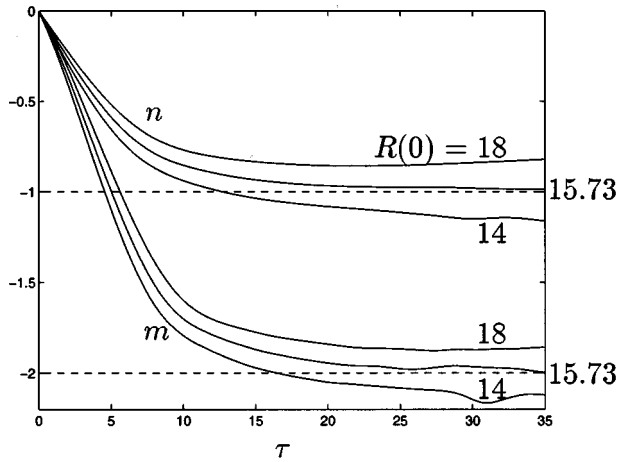


FIG. 2. Evolution of the logarithmic derivative of the energy ( $n$ ) and enstrophy ( $m$ ) for  $R(0)=14, 15.73$  and  $18$ .

approached asymptotically inasmuch that  $n$  and  $m$  approach  $-2$  and  $-3$ , respectively, at large times. Strong deviations from these asymptotic power-law exponents at the latest times simulated is due to finite size effects of the periodic box, so that (17) is no longer valid.

It is of interest to consider somewhat larger initial Reynolds numbers. These simulation results are of  $2048^2$  resolution with  $k_p=300$  in (11). Results for the logarithmic derivatives of the energy and enstrophy with  $R(0)=14, 15.73$ , and  $18$  versus  $\tau$  are shown in Fig. 2. The corresponding Reynolds numbers  $R(t)$  versus  $\tau$  are shown in Fig. 3. Our numerical experiments demonstrate the existence of a critical Reynolds number  $R_c \approx 15.73$  such that for  $R(0) < R_c$  the Reynolds number decays monotonically in time and for  $R > R_c$  the Reynolds number decreases initially, and then increases asymptotically. Results for initial Reynolds numbers  $R(0)=14, 18$  are shown in Figs. 2 and 3 for comparison purposes. At  $R(0)=R_c$ , the numerical simulation results

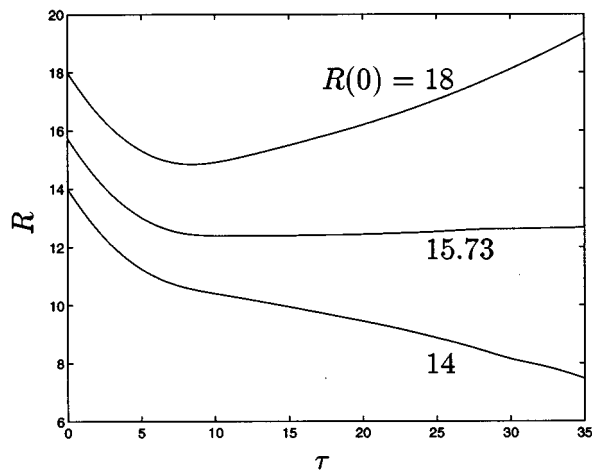


FIG. 3. Time evolution of the Reynolds number  $R$  for  $R(0)=14, 15.73$  and  $18$ .

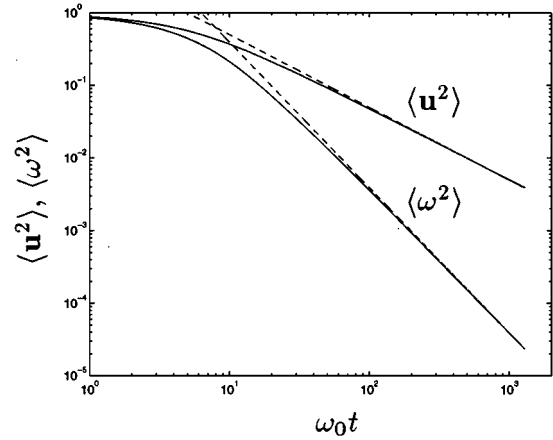


FIG. 4. Time evolution of the energy and enstrophy for  $R(0)=15.73$  compared to the analytical results of (23).

yield an approximate power-law decay of the energy as  $t^{-1}$ , and an approximate enstrophy decay as  $t^{-2}$ .

An analytical derivation of these power-law exponents is possible by assuming that the energy and enstrophy decay as power laws, and that the Reynolds number approaches a time-independent constant, here taken to be  $R'_c$ , at large times. Writing

$$\langle \mathbf{u}^2 \rangle = bt^n, \quad \langle \omega^2 \rangle = ct^m, \quad (22)$$

one has from the definition of the Reynolds number (13) the equations  $n=m/2$  and  $b = \nu R'_c \sqrt{c}$ . Furthermore, the energy equation (3) yields the equations  $n-1=m$  and  $nb = -2\nu c$ . Solving, one thus obtains the asymptotic solution at  $R(0)=R_c$ :

$$\langle \mathbf{u}^2 \rangle = \frac{1}{2} \nu R'_c{}^2 t^{-1}, \quad \langle \omega^2 \rangle = \frac{1}{4} R'_c{}^2 t^{-2}. \quad (23)$$

In Fig. 4, the energy and enstrophy decay for  $R(0)=15.73$  is compared to the analytical results (23), where we have taken  $R'_c = 12.5$  as approximately determined from Fig. 3. The simulation results and analytical solution are in good agreement at large times. Interestingly, the Batchelor decay law  $t^{-2}$  for the enstrophy is found by assuming a flow field which decays at constant Reynolds number. The energy however is no longer constant but decays as  $t^{-1}$ .

When  $R(0) > R_c$ , the Reynolds number  $R(t)$  increases asymptotically, and it is of interest to consider whether another different similarity state develops. It is plausible that a unique similarity state exists since all flows with initial Reynolds numbers greater than  $R_c$  presumably approach infinite Reynolds numbers as  $t \rightarrow \infty$ . Calculations for a range of  $R(0) > R_c$  will be presented in the next section to test the possibility of a unique similarity state.

#### IV. SIMULATIONS AT HIGH REYNOLDS NUMBERS

We now present the results of direct numerical simulations of two-dimensional turbulence decay with initial Reynolds numbers ranging from  $R(0)=32$  to  $4096$ . The simulations have been performed so that the small scales of the turbulence are adequately resolved and finite size effects as-

sociated with the computational box may be neglected. The calculations were checked for accuracy by varying both the resolution and the wave number  $k_p$  at which the initial energy spectrum (11) is maximum. The simulations presented are at resolution  $4096^2$  and the initial energy spectrum is chosen with  $u_0=1$  and with  $k_p$  ranging from 600 to 16 as the initial Reynolds number increases from 32 to 4096. The total computational cost of the calculation grows with decreasing  $k_p$  due to the increasing number of time steps required for a complete calculation.

The time evolution of  $(2\times)$  the energy, enstrophy, and palinstrophy, normalized using  $u_0$ ,  $\omega_0$  and  $l_0$ , (15), for the different values of  $R(0)$  are shown in Fig. 5. The energy and enstrophy decay monotonically in time as required from (3) and (4), while the palinstrophy increases to a maximum before beginning to decay.

The logarithmic derivatives of the energy and enstrophy (19) versus  $\tau$  (21) are plotted in Fig. 6. No universal decay exponent of the enstrophy, Fig. 6(b), at large times for all initial Reynolds numbers greater than  $R_c$  is observed. However, for  $R(0)\geq 1024$  the long-time decay exponent appears to change only slightly and the asymptotic decay law for these large Reynolds numbers follows approximately  $t^{-0.8}$ . These high Reynolds number flows are nearly inviscid in so much that the energy, Fig. 5(a), decays very little over the times simulated.

The logarithmic derivative of the energy  $n$ , Fig. 6(a), is observed to be an increasing function of the initial Reynolds number, indicating that the energy decay becomes less steep with increasing initial Reynolds numbers. This is also readily evident from the energy decay itself, Fig. 5(a). We further comment on the different qualitative behavior of  $n$  at low and high initial Reynolds numbers. For relatively low initial Reynolds numbers ( $R(0)<256$ ),  $n$  decreases to a minimum and then increases in time. This signifies a rapid initial decay of the energy which subsequently becomes less steep as time evolves, presumably due to the increasing Reynolds number of the turbulence. For  $R(0)>256$ , however,  $n$  slowly decreases in time implying that the energy decay is steepening as time evolves. However, the magnitude of  $n$  for these high Reynolds numbers is quite small, and the energy does not decay significantly over the times simulated. Since the energy is related to the time integral of the enstrophy, the change in the qualitative behavior of the logarithmic derivative of the energy coincides with the power-law exponent of the enstrophy increasing from less than to greater than negative one.

One obvious point is evident from the simulation results presented in Fig. 6(b): the enstrophy at high Reynolds numbers does not decay as  $t^{-2}$  as predicted by Batchelor.<sup>4</sup> Previous investigations have already recognized this. Arguing on the basis of observed coherent vortices in two-dimensional decay, Carnevale *et al.*<sup>2</sup> proposed the existence of a second conserved quantity in addition to the energy. From numerical solutions of vortex merging, a decay of the enstrophy proportional to  $t^{-0.37}$  was proposed. An enstrophy decay ranging from  $t^{-0.29}$  to  $t^{-0.35}$  was determined in nearly inviscid calculations of Dritschel,<sup>3</sup> who also suggested that the decay exponents may depend strongly on the initial con-

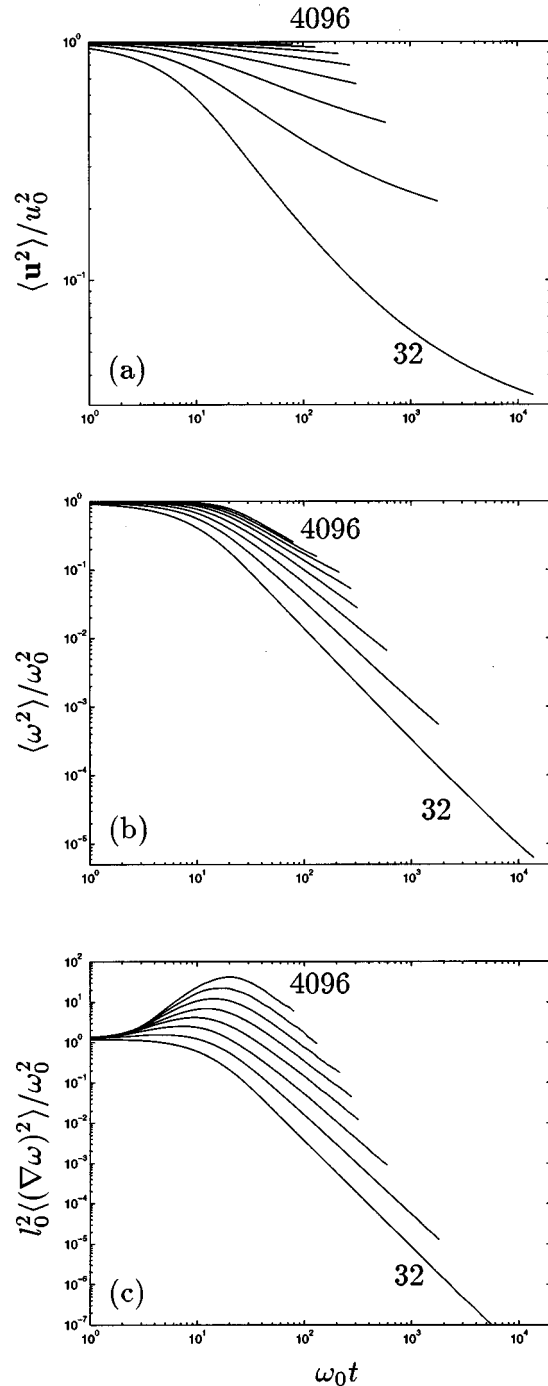


FIG. 5. Time evolution of the statistics for  $R(0)=32, 64, \dots, 4096$ . (a) Energy; (b) enstrophy; (c) palinstrophy.

ditions of the flow field as well as the Reynolds number. It is unclear why our large Reynolds number decay law of the enstrophy as  $t^{-0.8}$  is substantially steeper than that determined by these previous investigations.

In Fig. 7(a), we plot the Reynolds number  $R(t)$  as a function of  $\omega_0 t$ . One observes that the Reynolds number increases asymptotically in time as expected. In Fig. 7(b), we also plot the flatness factor of the vorticity, defined as

$$f(t) = \frac{\langle \omega^4 \rangle}{\langle \omega^2 \rangle^2}, \quad (24)$$

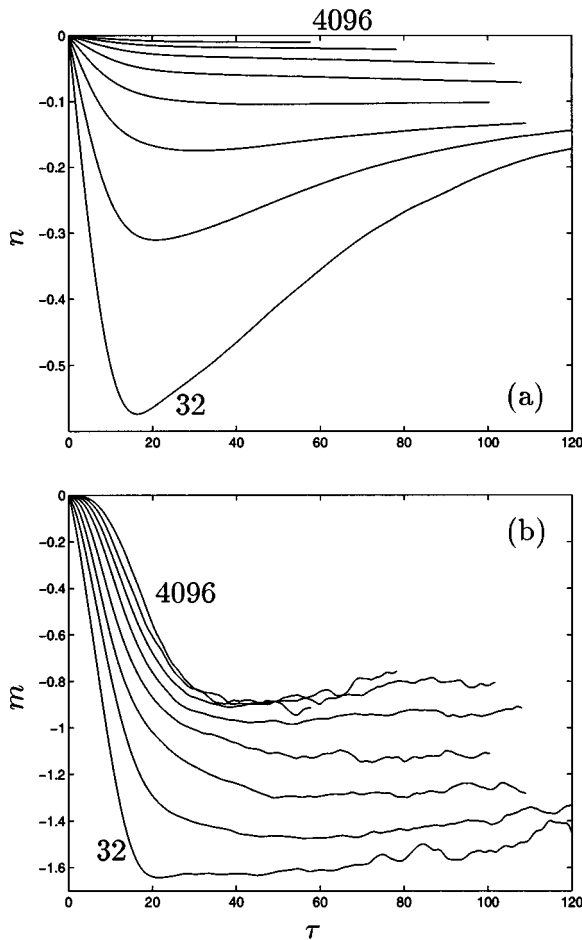


FIG. 6. Time evolution of the logarithmic derivative of the energy and enstrophy for  $R(0)=32,64,\dots,4096$ . (a) energy; (b) enstrophy.

versus  $\omega_0 t$ . The statistic  $f(t)$  has previously been used to characterize the spatial intermittency of the vorticity field.<sup>11,12</sup> Our random phase initial condition (12) corresponds to a flatness factor of three. The flatness factor also apparently increases without bound during the decay when  $R(0) > R_c$ . When  $R(0) = R_c$  (not shown),  $f(t)$  remains at approximately three. The occurrence of large values of the flatness factor during the decay of high Reynolds number two-dimensional turbulence has been previously observed, and it has been suggested that these large values are associated with the formation of coherent vortices, and furthermore that these vortices are responsible for the deviation from Batchelor scaling.<sup>11</sup>

## V. SCALING LAWS

The most puzzling feature of our high Reynolds number simulation results is the apparent lack of a unique asymptotic similarity state for two-dimensional turbulence for all initial Reynolds numbers greater than  $R_c$  even though these flows approach infinite Reynolds number asymptotically. Rather, different qualitative decay laws are observed for different ranges of initial Reynolds numbers and we will show here

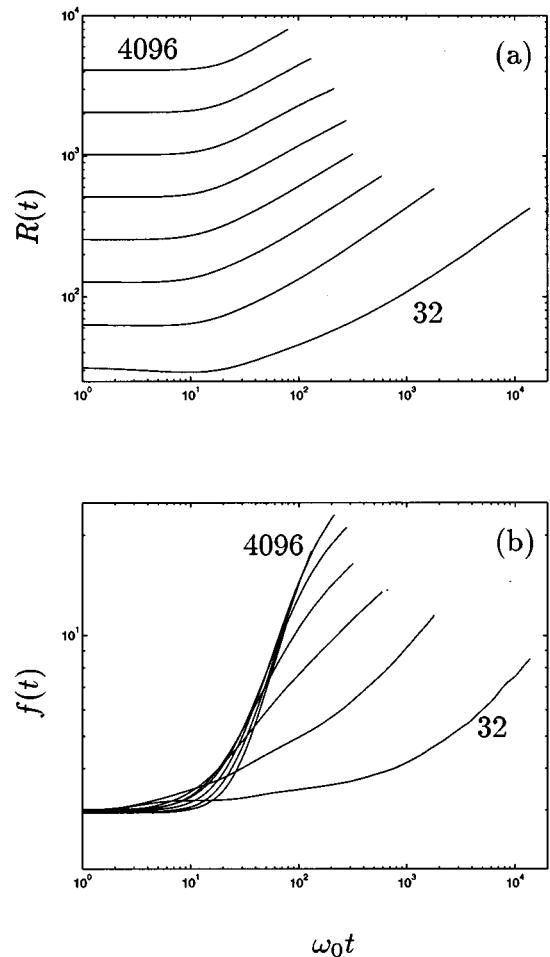


FIG. 7. Time evolution of the Reynolds number  $R(t)$  and vorticity flatness factor  $f(t)$  for  $R(0)=32,64,\dots,4096$ . (a)  $R(t)$ ; (b)  $f(t)$ .

that it is possible to fit the data over limited Reynolds number ranges by assuming different forms for the energy and enstrophy decay.

Our starting point is the energy equation (3), and the assumption of power-law forms (22) for the energy and the enstrophy. Substituting (22) into (3), one trivially obtains coupled equations for the exponents and coefficients:

$$n - 1 = m, \quad nb = -2\nu c. \quad (25)$$

An energy which approaches a constant asymptotically as the Reynolds number becomes large would require  $n=0$  asymptotically which does not satisfy (25) for  $\nu > 0$ . Of course, it is always possible to add a constant to the power-law decay of the energy as found in (6), and the enstrophy (5) is then related to the energy through the next-order term in  $(1/t)$ . Here, however, we take a different approach and consider that a solution with  $n=0$  can also be obtained if one considers an additional (ad-hoc) logarithmic correction to the power-law ansatz of (22). With  $n=0$ , one thus replaces (22) by the form

$$\langle \mathbf{u}^2 \rangle = u_*^2 [\log(t/t_*)]^p, \quad p < 0; \quad (26)$$

and the energy equation (3) then yields for the enstrophy

TABLE I. Fitted parameter values obtained from (29) and used in Fig. 8.

$R(0)$	$u_*$	$t_*$	$u_*^2 t_* / \nu$
32	0.29	217	590
64	0.77	17	650

$$\langle \omega^2 \rangle = \frac{-p u_*^2}{2\nu} t^{-1} [\log(t/t_*)]^{p-1}. \quad (27)$$

A logarithmic decay of the energy implies an enstrophy decay as  $t^{-1}$  asymptotically with a logarithmic correction.

The solution given by (26) and (27) is physically appealing in that the energy decay becomes less and less steep as the Reynolds number increases during the decay, yet the energy never completely escapes dissipation by viscosity as occurs in (6). This behavior of the energy decay seems to agree with that observed from the simulation data for  $R_c < R(0) < 256$ . However, for fixed  $t$  as  $\nu \rightarrow 0$ , the solution given by (26) and (27) is incorrect since in this limit the energy should become constant. To obtain a solution in which the energy becomes constant as  $\nu \rightarrow 0$ , it is possible to return to the original ansatz (22) and solve (25) directly for the power-law exponents  $n$  and  $m$  in terms of the assumed constant coefficients  $b$  and  $c$ . In this fashion, one obtains the solutions

$$\langle \mathbf{u}^2 \rangle = b t^{-2\nu c/b}, \quad \langle \omega^2 \rangle = c t^{-(1+2\nu c/b)}. \quad (28)$$

Here, for fixed  $t$  as  $\nu \rightarrow 0$  one has  $\langle \mathbf{u}^2 \rangle \rightarrow b = u_0^2$ ; and the enstrophy again decays as  $t^{-1}$ . As mentioned in the introduction, there are no finite time singularities in two-dimensional turbulence as  $\nu \rightarrow 0$ , so that (28) is still incorrect in that the enstrophy should approach a constant in this limit but does not.

The numerical simulation results for the logarithmic derivatives of the energy and enstrophy shown in Fig. 6 show a sharp minimum in the power-law exponent of the energy for the initial Reynolds numbers  $R(0) = 32, 64$ . We now show that (26) and (27) can provide a good fit to the energy and enstrophy decay with proper choices of  $p$ ,  $u_*$ , and  $t_*$ . These parameters may be fitted to the data using the computed values for the logarithmic derivatives of the energy and enstrophy, as well as (19), (26) and (27). The relations we use to fit the parameters are

$$p = \frac{n}{n-m-1}, \quad t_* = t \exp\left(\frac{-1}{n-m-1}\right), \quad (29)$$

$$u_*^2 = \langle \mathbf{u}^2 \rangle (n-m-1)^{n/(n-m-1)}.$$

We have determined that a good fit to the simulation data for  $R(0) = 32, 64$  can be obtained with a value of  $p = -2/3$ . The other values of  $u_*$ ,  $t_*$ , and the nondimensional group  $u_*^2 t_* / \nu$  are shown in Table I. The nondimensional group  $u_*^2 t_* / \nu$  can be considered to be the time  $t_*$  after which the log decay law is established normalized by a viscous time scale formed from  $u_*$  and  $\nu$ . The 10% variation of  $u_*^2 t_* / \nu$  over the two Reynolds number runs compared to the more than order-of-magnitude variation in  $t_*$  suggests that the logarithmic decay law of the energy is being established over

a time proportional to the viscous time scale. A plot of the simulation results for the energy and enstrophy decay compared to the analytical forms (26) and (27) is shown in Fig. 8, and very good agreement at large times between the simulation data and the analytical form is observed.

At higher-Reynolds numbers, the forms for the energy and enstrophy decay given by (26) and (27) no longer agree with the data. Examining the graph of the logarithmic derivative of the energy, Fig. 6(a), one observes that at  $R(0) = 256$ , the logarithmic derivative of the energy is approximately constant at large times, indicating a power-law decay for the energy. For smaller initial Reynolds numbers, the energy decay exponent is decreasing in magnitude, whereas for larger initial Reynolds numbers, the exponent is increasing in magnitude. The analytical form given by (28) may be fit to the simulation results for  $R(0) = 256$ , with the decay exponent of the energy given by  $n = -0.1$ . A comparison between the simulation result for  $R(0) = 256$  and the analytical form (28) is shown in Fig. 9, and reasonable agreement at large times is evident.

It appears from the results above that for  $R(0) < 256$ , the decay of the energy by viscous forces is determining both the asymptotic decay laws of the energy and enstrophy. This seems to be the case even though the Reynolds number of the flow field is increasing asymptotically. For initial Reynolds numbers larger than approximately 1024, viscous effects are much less important over the times simulated and the small amount of energy which does dissipate is of no apparent consequence. A nearly inviscid decay law of the enstrophy of approximately  $t^{-0.8}$  is then observed from the simulation data. We have no theoretical explanation for this exponent value.

## VI. SPECTRA

We now consider whether the energy spectrum  $E(k, t)$  of two-dimensional turbulence decays self-similarly, that is, without change of shape. For flows with  $R(0) > R_c$ , self-

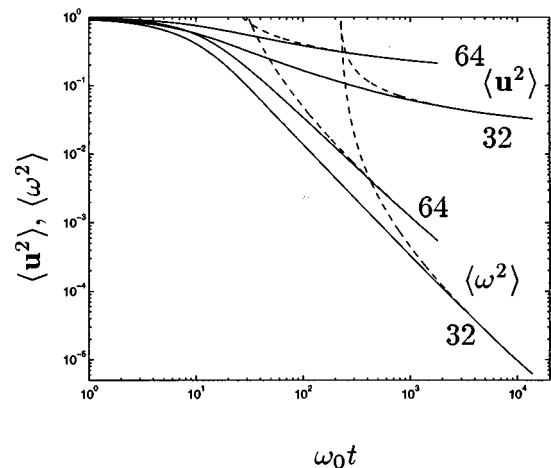


FIG. 8. Time evolution of the energy and enstrophy for  $R(0) = 32, 64$  compared to the analytical forms of (26) and (27).

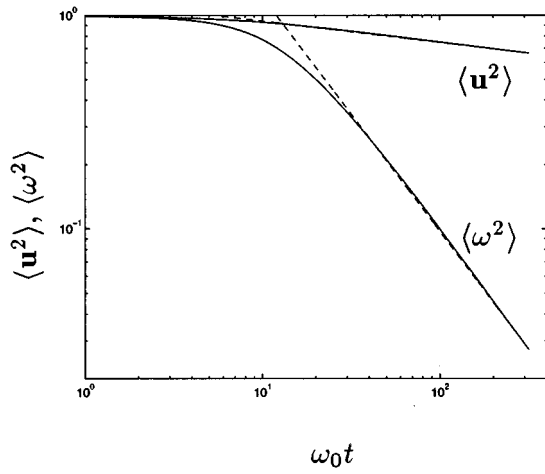


FIG. 9. Time evolution of the energy and enstrophy for  $R(0)=256$  compared to the analytical forms of (28).

similarity of the spectrum for all wave numbers is impossible due to the increase of the Reynolds number in time. However, for  $R(0)=R_c$  a self-similar decay of the entire spectrum can occur. We define a self-similar energy spectrum  $\hat{E}(\hat{k})$  from

$$E(k,t) = u^2 l \hat{E}(\hat{k}), \quad \hat{k} = kl, \quad (30)$$

where the velocity and length scales  $u$  and  $l$  are defined in (14). In plotting the spectrum itself, we also normalize using  $u_0$  and  $l_0$  defined in (15).

In Fig. 10, the time evolution of the nondimensional energy spectrum  $E(k)/u_0^2 l_0$  for  $R(0)=15.73$  versus nondimensional wave number  $kl_0$  for  $\tau=0,5,10,\dots,35$  is plotted. To test whether the spectrum is decaying self-similarly,  $\hat{E}(\hat{k})$  versus  $\hat{k}$  is plotted in Fig. 11 for  $\tau=10,15,\dots,35$  using (30). A near-perfect collapse of  $\hat{E}(\hat{k})$  at the different times plotted is observed indicating a self-similar decay of the spectrum

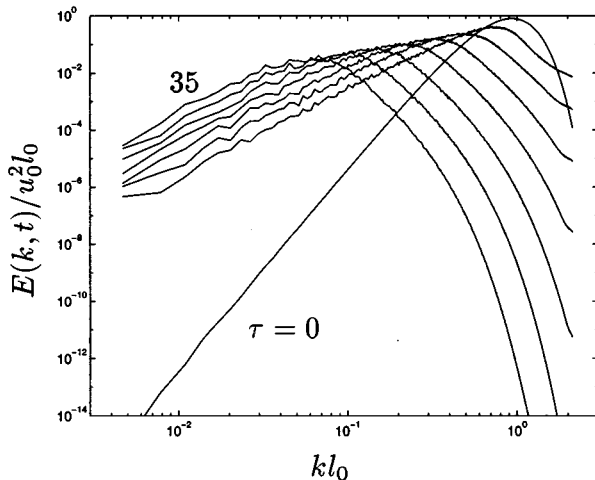


FIG. 10. Evolution of the normalized energy spectrum in time with  $R(0)=15.73$ . The times plotted correspond to  $\tau=0,5,10,\dots,35$ .

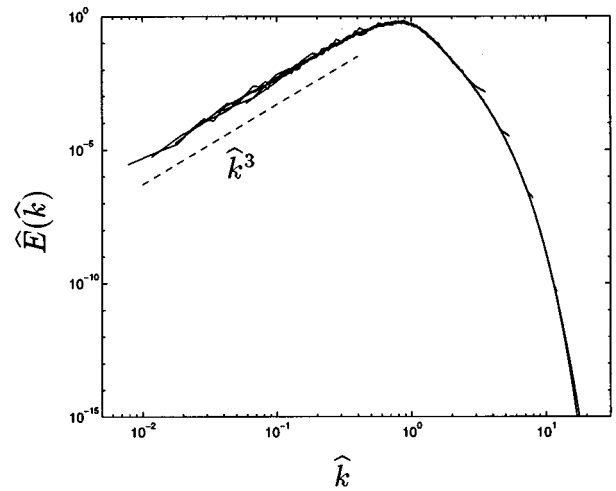


FIG. 11. Rescaling of the energy spectrum of Fig. 10. The times plotted correspond to  $\tau=10,15,\dots,35$ .

over all wave numbers. Also observe that the characteristic  $B_2(t)k^3$  spectrum of (17) is clearly evident at low wave numbers. Self-similarity of the spectrum given by (30) and the low wave number form of the spectrum (17) results in the scaling

$$B_2(t) \propto u^2 l^4; \quad (31)$$

and when  $R(0)=R_c$ , the analytical decay laws given by (23) yield

$$B_2(t) \propto \nu^3 R_c'^2 t; \quad R(0)=R_c. \quad (32)$$

The low wave number coefficient of the spectrum  $B_2(t)$  thus increases linearly in time, indicating substantial nonlinear backscatter of energy from small-to-large scales even for this low Reynolds number turbulence. Recall that  $B_2(t)$  is independent of time within a linear analysis.

Next we consider the time evolution of the energy spectra for flows with  $R(0)>R_c$ . In particular, the time evolution of the spectra for  $R(0)=64, 256,$  and  $4096$  are shown in Fig. 12. The times  $\tau$  which are plotted are written in the figure caption. Note how we have positioned the peak of the initial energy spectrum in wave number space at the largest possible (dimensional) wave number which provides adequate small-scale resolution for a given initial Reynolds number. This reduces the computational cost of each calculation as well as provides the best possible statistical sample of the largest vortices in a single realization. In Fig. 13, the self-similar spectra obtained using (30) are plotted.

It appears from the reasonable collapse of the spectra at different times evident from Fig. 13 that the decay of two-dimensional turbulence at large Reynolds number is also self-similar in the energy containing scales. One should observe however that the spectra of the viscous scales at the largest wave numbers do not collapse due to the increasing Reynolds number of the turbulence during the decay. This is particularly evident for  $R(0)=64$ , Fig. 13(a). The collapse at the smallest wave numbers is also not as good as observed for  $R(0)=15.73$ , Fig. 11, though it is impossible to say from our data whether this is only due to a lack of adequate sta-



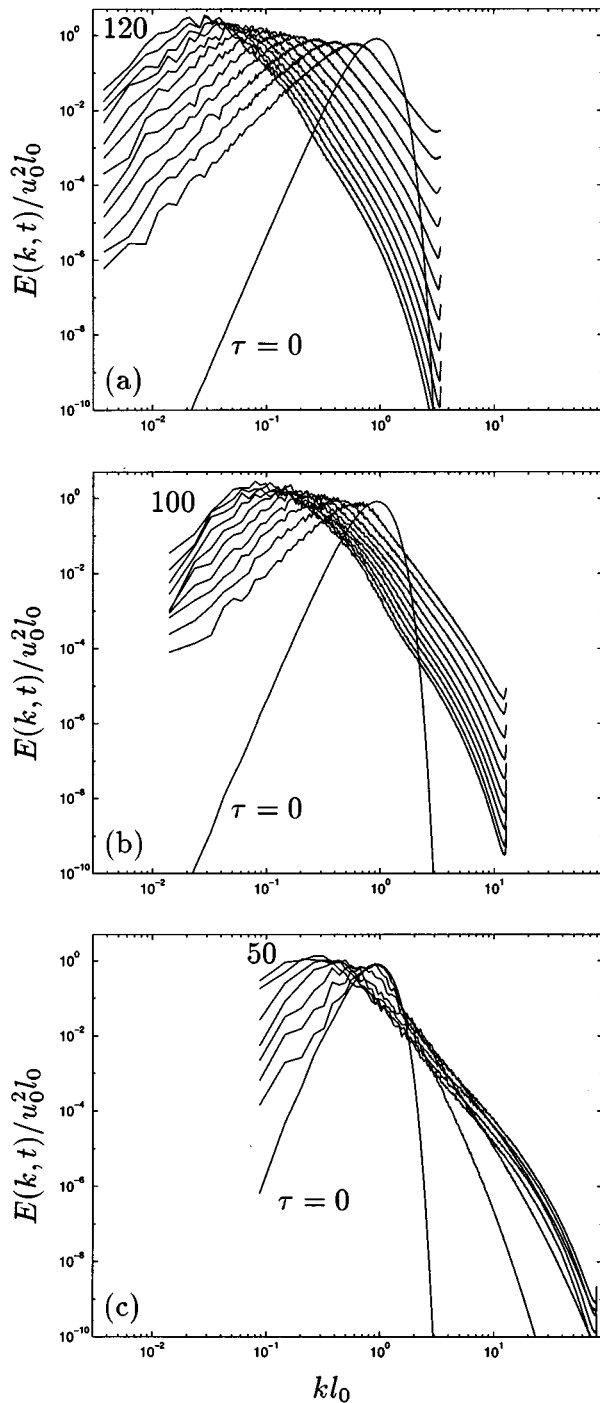


FIG. 12. Evolution of the energy spectrum in time. (a)  $R(0)=64$ ,  $\tau=0, 10, 20, \dots, 120$ ; (b)  $R(0)=256$ ,  $\tau=0, 10, 20, \dots, 100$ ; (c)  $R(0)=4096$ ,  $\tau=0, 2.5, 10, 20, \dots, 50$ .

tistical sample of the largest vortices. In Fig. 13, we have also plotted as a dashed line the expected  $\hat{k}^3$  low wave number behavior, as well as the predicted<sup>5,13,14</sup>  $\hat{k}^{-3}$  inertial subrange behavior for two-dimensional turbulence. At the highest Reynolds numbers, Fig. 13(c), an inertial subrange appears to have developed which is slightly steeper than the predicted power-law behavior.

If indeed the spectrum decays self-similarly at low wave numbers, it is possible to derive a relationship between the

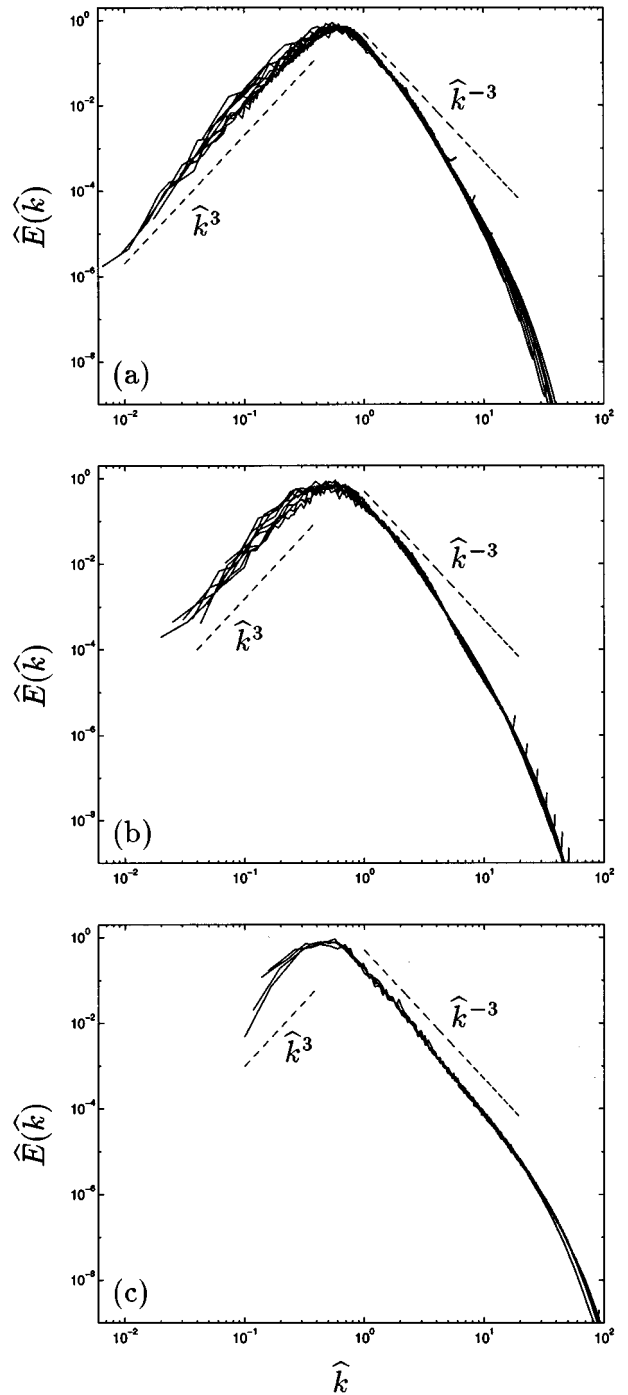


FIG. 13. Rescaling of the energy spectra of Fig. 12. (a)  $R(0)=64$ ,  $\tau=20, 30, \dots, 120$ ; (b)  $R(0)=256$ ,  $\tau=20, 30, \dots, 100$ ; (c)  $R(0)=4096$ ,  $\tau=20, 30, \dots, 50$ .

enstrophy and the low wave number spectral coefficient  $B_2(t)$  using (31) and the near-invariance of  $u(t)=u_0$ :

$$\langle \omega^2 \rangle \propto \frac{u_0^3}{\sqrt{B_2(t)}}. \quad (33)$$

Equation (33) suggests that the nonlinear backscatter of energy from small-to-large scales as represented by the time dependence of  $B_2(t)$  may be the relevant physics which determines the precise time-decay law of the enstrophy. An

enstrophy decay of approximately  $t^{-0.8}$  corresponds to  $B_2(t) \propto t^{1.6}$ , which is somewhat more rapid than the linear increase (32) at low Reynolds numbers when  $R(0)=R_c$ . Batchelor's original self-similarity hypothesis based on the invariance of  $u_0$  at high Reynolds numbers results in the more rapid growth  $B_2(t) \propto u_0^6 t^4$ , and apparently standard closure approximations agree with this estimate.<sup>8</sup>

## VII. CONCLUSIONS

The main contribution of this work is to provide detailed statistical results from direct numerical simulations of decaying two-dimensional homogeneous turbulence at varying initial Reynolds numbers. The existence of a critical Reynolds number is established below which the turbulence enters a final period of decay, and above which the turbulence evolves with asymptotically increasing Reynolds number. However, even though all flows with initial Reynolds numbers above  $R_c$  evolve to high Reynolds numbers, no unique universal asymptotic state is observed. Rather, we have indicated different ranges in initial Reynolds numbers where various scaling behaviors are found. Only at relatively high initial Reynolds numbers when the energy decay is apparently negligible over the times simulated does the enstrophy decay seem to approach a universal decay law of approximately  $t^{-0.8}$ .

We have also further determined a self-similar decay of the turbulence energy spectrum. The self-similarity is apparently exact for  $R(0)=R_c$  but is necessarily approximate for  $R(0)>R_c$  due to the increase of the Reynolds number during the decay. At the highest Reynolds number simulated, an enstrophy-cascading inertial subrange of almost one decade is observed. Finally, we comment that our numerical simulations seem to yield widely different results for the energy and enstrophy decay than closure approximations,<sup>7,8</sup> even though many characteristics of the energy spectra are the same, including a  $k^3$  form at low wave numbers and a near  $k^{-3}$  inertial subrange at high wave numbers, as well as a self-similar decay of the spectra in time.

## ACKNOWLEDGMENTS

I wish to thank L. Smith and F. Waleffe for many stimulating discussions, and J. Herring and R. Rogallo for their comments. I also wish to thank A. Wray and R. Rogallo for making their software freely available. The support of the Hong Kong Research Grant Council is gratefully acknowledged. The computations presented here were performed on an Intel Paragon at The Hong Kong University of Science & Technology.

- <sup>1</sup>J. C. McWilliams, "The vortices of two-dimensional turbulence," *J. Fluid Mech.* **219**, 361 (1990).
- <sup>2</sup>G. F. Carnevale, J. C. McWilliams, Y. Pomeau, J. B. Weiss, and W. R. Young, "Rates, pathways, and end states of nonlinear evolution in decaying two-dimensional turbulence: Scaling theory versus selective decay," *Phys. Fluids A* **4**, 1314 (1992).
- <sup>3</sup>D. G. Dritschel, "Vortex properties of two-dimensional turbulence," *Phys. Fluids A* **5**, 984 (1993).
- <sup>4</sup>J. R. Chasnov, "Similarity states of passive scalar transport in isotropic turbulence," *Phys. Fluids* **6**, 1036 (1994).
- <sup>5</sup>G. K. Batchelor, "Computation of the energy spectrum in homogeneous two-dimensional turbulence," *Phys. Fluids Suppl. II* **12**, 233 (1969).
- <sup>6</sup>A. Pouquet, M. Lesieur, J. C. Andre, and C. Basdevant, "Evolution of high Reynolds number two-dimensional turbulence," *J. Fluid Mech.* **72**, 305 (1975).
- <sup>7</sup>T. Tatsumi and S. Yanase, "The modified cumulant expansion for two-dimensional isotropic turbulence," *J. Fluid Mech.* **110**, 475 (1981).
- <sup>8</sup>M. Lesieur, *Turbulence in Fluids* (Kluwer, Dordrecht, 1990).
- <sup>9</sup>M. E. Brachet, M. Meneguzzi, H. Politano, and P. L. Sulem, "The dynamics of freely decaying two-dimensional turbulence," *J. Fluid Mech.* **194**, 333 (1988).
- <sup>10</sup>R. S. Rogallo and A. Wray (private communication).
- <sup>11</sup>J. R. Herring and J. C. McWilliams, "Comparison of direct numerical simulation of two-dimensional turbulence with two-point closure: The effect of intermittency," *J. Fluid Mech.* **153**, 229 (1985).
- <sup>12</sup>L. M. Smith and V. Yakhot, "The onset of intermittency in two-dimensional decaying turbulence," *Phys. Rev. E* (submitted).
- <sup>13</sup>R. H. Kraichnan, "Inertial ranges in two-dimensional turbulence," *Phys. Fluids* **10**, 1417 (1967).
- <sup>14</sup>R. H. Kraichnan, "Inertial range transfer in two- and three-dimensional turbulence," *J. Fluid Mech.* **47**, 525 (1971).